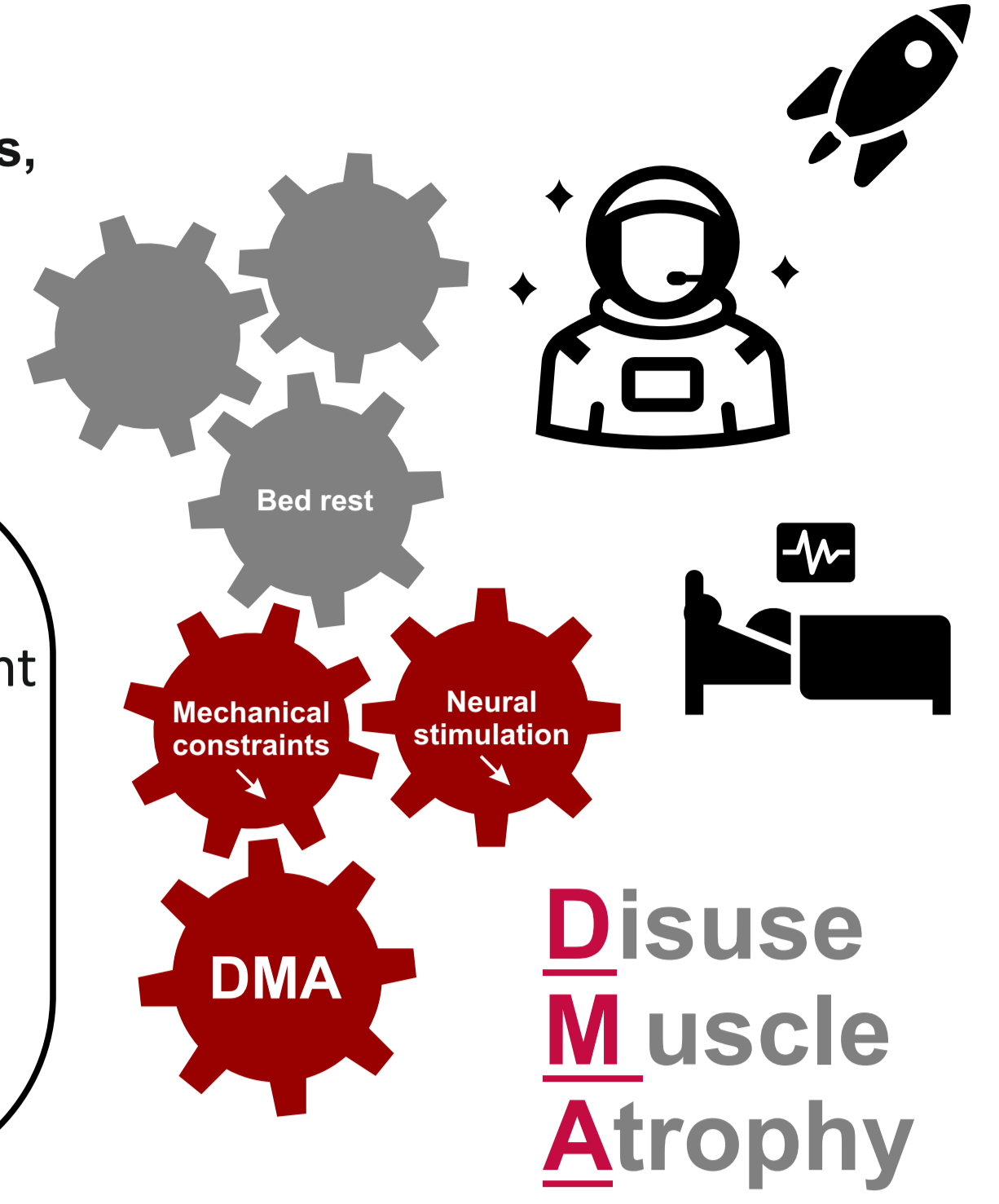


Adiponectin pathway in a murine models of skeletal muscle deconditioning and reconditioning

S. Szczepanski¹, M. Limpens¹, V. Blommaert¹, V. Jenart¹, A. Legrand¹, A-E. Declèves², A. Tassin¹
 1. Lab. Respiratory Physiology, Pathophysiology and Rehabilitation, Research Institute for Health Sciences and Technology, University of Mons,
 2. Lab. Metabolic and Molecular Biochemistry, Research Institute for Health Sciences and Technology, University of Mons



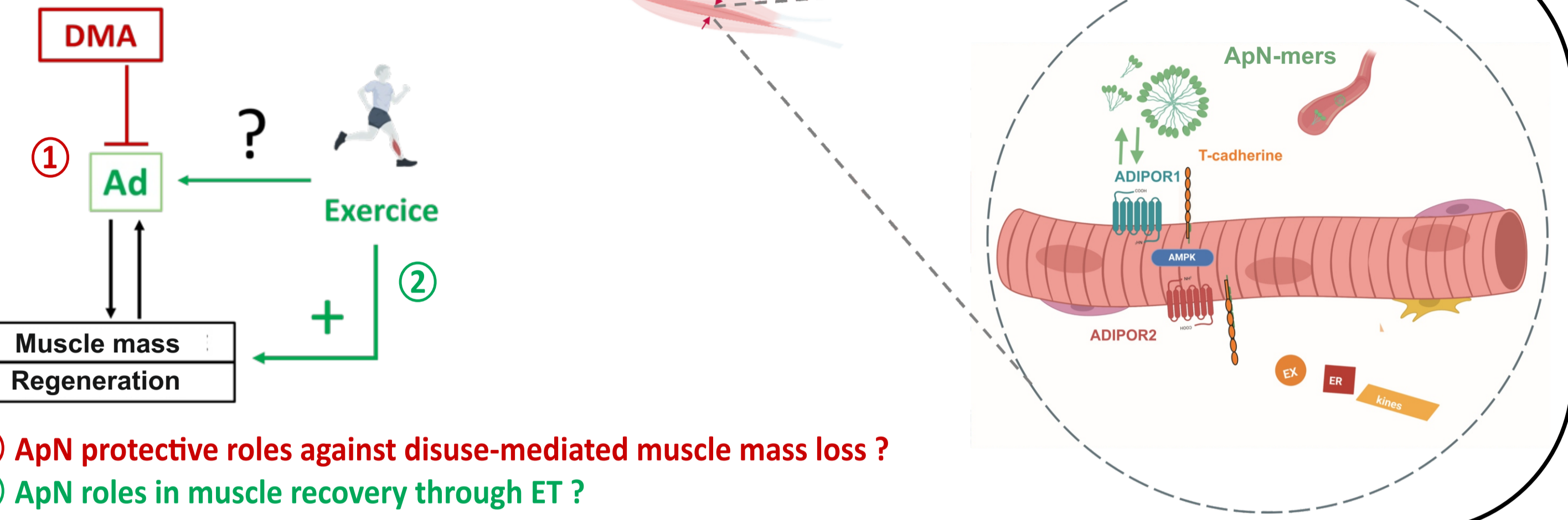
Introduction

Skeletal muscle deconditioning is an important issue for patients managed in Intensive-Care Unit (ICU) where prolonged bedrest results in the development of a Disuse-mediated Muscle Atrophy (DMA) associated to an impaired regeneration compromising muscle recovery (Baehr L et al., Cell, 2022). While exercise training (ET) is the only effective treatment against DMA, ET intolerance limits rehabilitation. As well, mechanisms and its beneficial effects must be clarified.

Skeletal muscle is an endocrine organ that secretes myokines and **exerkines** are those that results from ET. Adiponectin (ApN) is an adipo/myokine with anti-inflammatory, antioxidant, and pro-myogenic properties. While increasing evidence highlights its positive role in skeletal muscle, ApN pathway was found altered in a murine model of DMA (Goto et al., PLoS ONE, 2013).

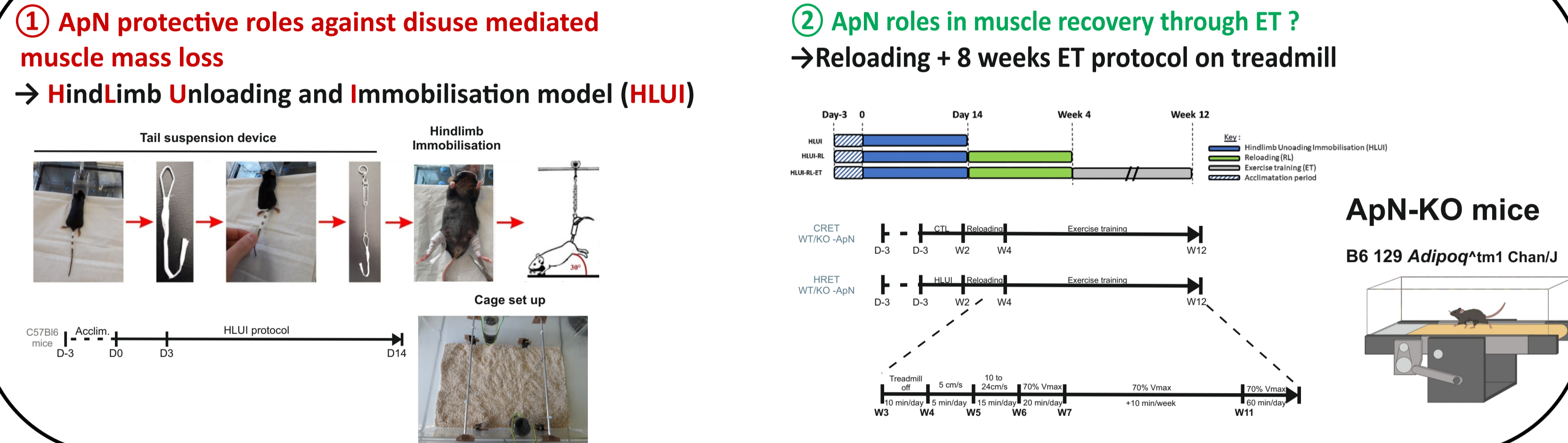
We hypothesize that muscle deconditioning is associated to ApN pathway alterations which could reinforce (i) the loss of muscle mass and (ii) the impairment of muscle regeneration in a vicious circle.

Aims



- ① ApN protective roles against disuse-mediated muscle mass loss ?
- ② ApN roles in muscle recovery through ET ?

Methods



Characterization of the HLUI model

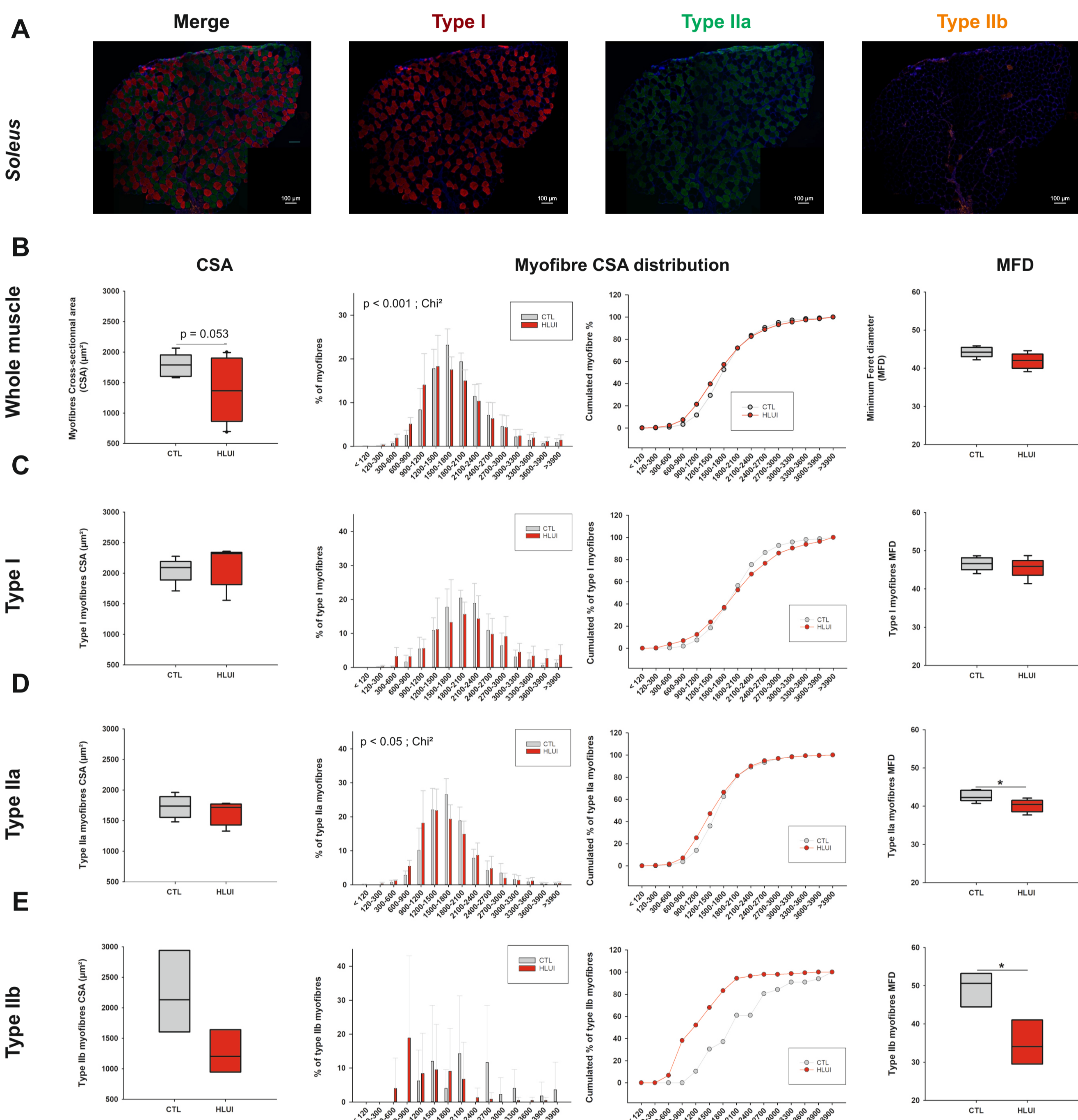


Figure 1. Effect of 14 days of Hindlimb Unloading coupled with Immobilization (HLUI) on mouse Soleus muscle: Cross-sectional Area (CSA), myofiber CSA distribution and Feret's diameter. Each myofiber CSA was measured on *Soleus* muscle cryosections following type I, IIa and IIb immunofluorescence detection and morphometric analyses performed with the *Image J* software. (A) Representative fields. (Left) CSA was measured in all fibres (B), in type I (C), in type IIa (D) and in type IIb fibres (E). Data represented as boxplot. t-test, NS. (Center) Myofibres were classified in clusters according to their area (μm^2). All fibres (B), type I fibres (C), type IIa fibres (D), and in type IIb fibres (E). Data represented as mean \pm SD. Chi-squared. Cumulative percentages of myofibres in clusters in all fibres (B), in type I (C), in type IIa (D) and in type IIb fibres (E). (Right) Minimum Feret's diameter (MFD) was measured in all fibres (B), in type I (C), in type IIa (D) and in type IIb fibres (E). Data represented as boxplot. *; $p < 0.05$; t-test.

Effect of HLUI on muscular components of ApN pathway

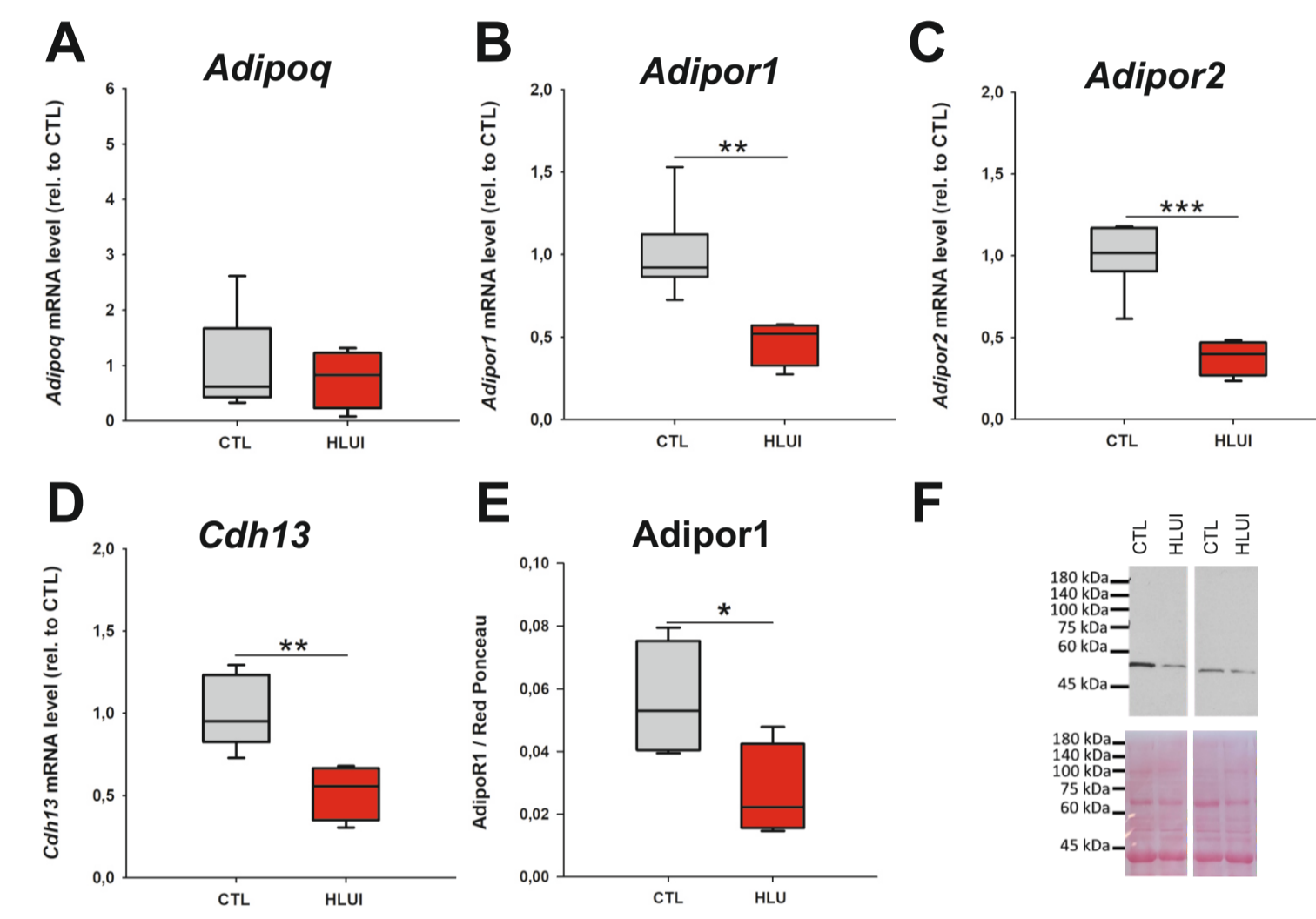


Figure 4. Effect of 14 days of HLUI on Adiponectin pathway in mouse Soleus muscle. (A-D) *Adipoq* (A), *Adipor1* (B), *Adipor2* (C) and *Cdh13* (D) mRNA level were assessed in the *Soleus* muscle by RTqPCR with $\Delta\Delta\text{Ct}$ method (housekeeping gene: *Rplp0*; data normalised to CTL). Data represented as boxplot; **; $p < 0.01$, ***; $p < 0.001$; t-test. (E) *Adipor1* protein level was determined in the *Soleus* muscle by Western blot. Data represented as boxplot; *; $p < 0.05$; t-test. (F) Representative blot.

Effect of ApN loss-of-function in HLUI mice submitted to ET

Figure 5. Ad knockout verification at the protein level in the plasma and at the mRNA level in the Gastrocnemius muscle of ApN-KO and WT mice following CRET or HRET protocol. (A) ApN plasmatic level was measured in the plasma of WT and AdKO mice following CRET or HRET protocol. Data represented as boxplot. *** $p < 0.001$, Two-way ANOVA, all pairwise multiple comparison (Holm-Sidak) (B) *Adipoq* mRNA level was assessed in the *gastrocnemius* muscle of WT and AdKO mice following CRET or HRET protocol with the $\Delta\Delta\text{Ct}$ method (*Rplp0* as housekeeping gene) and normalised to WT-CRET (Control). Data represented as boxplot. *** $p < 0.001$, Two-way ANOVA, all pairwise multiple comparison (Holm-Sidak).

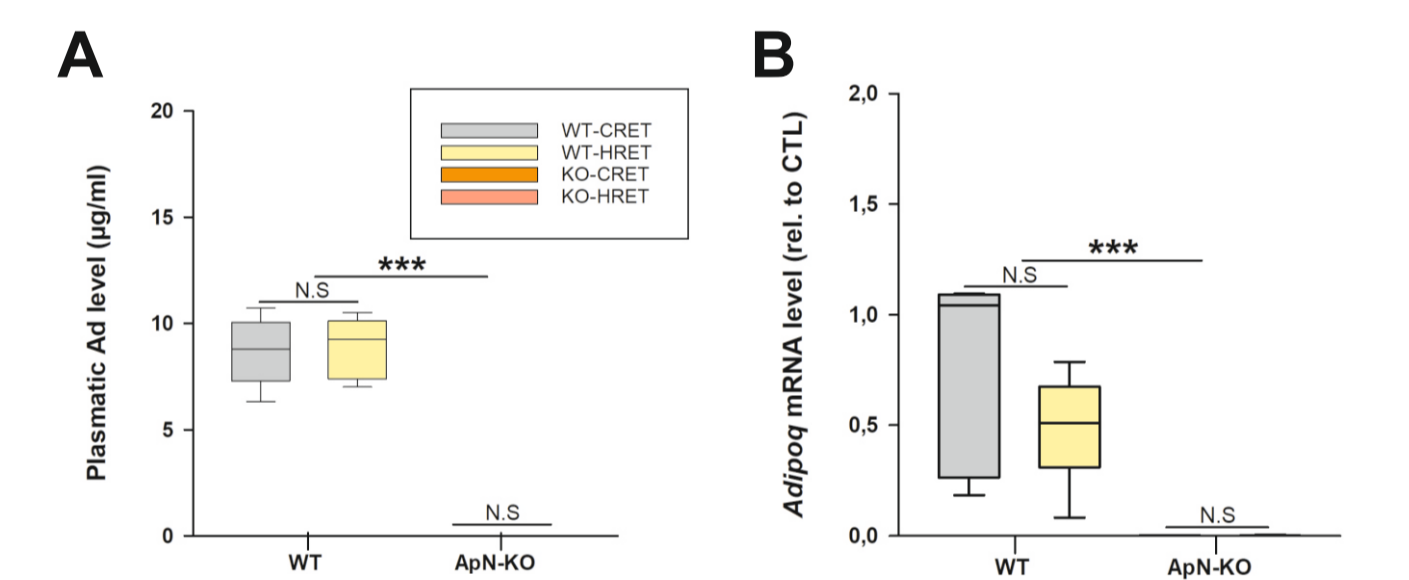


Figure 6. Effect of HLUI followed or not by ET on mouse Soleus muscle CSA in WT and ApN-KO mice. (A) Myofiber CSA was measured in all, in type I and in type IIa myofibres on *Soleus* muscle in WT and ApN-KO mice after CTL or HLUI protocol. Data represented as boxplot. *; $p < 0.05$ (protocol effect, KO-CTL vs KO-HLUI), $p < 0.05$ (protocol effect, CTL vs HLUI). Two Way ANOVA, Holm Sidak method. (B) CSA was measured in all, in type I and in type IIa myofibres on *Soleus* muscle in WT and ApN-KO mice after CRET or HRET protocol. Data represented as boxplot. *; $p < 0.05$, Two Way ANOVA.

Effect of HLUI on plasmatic ApN

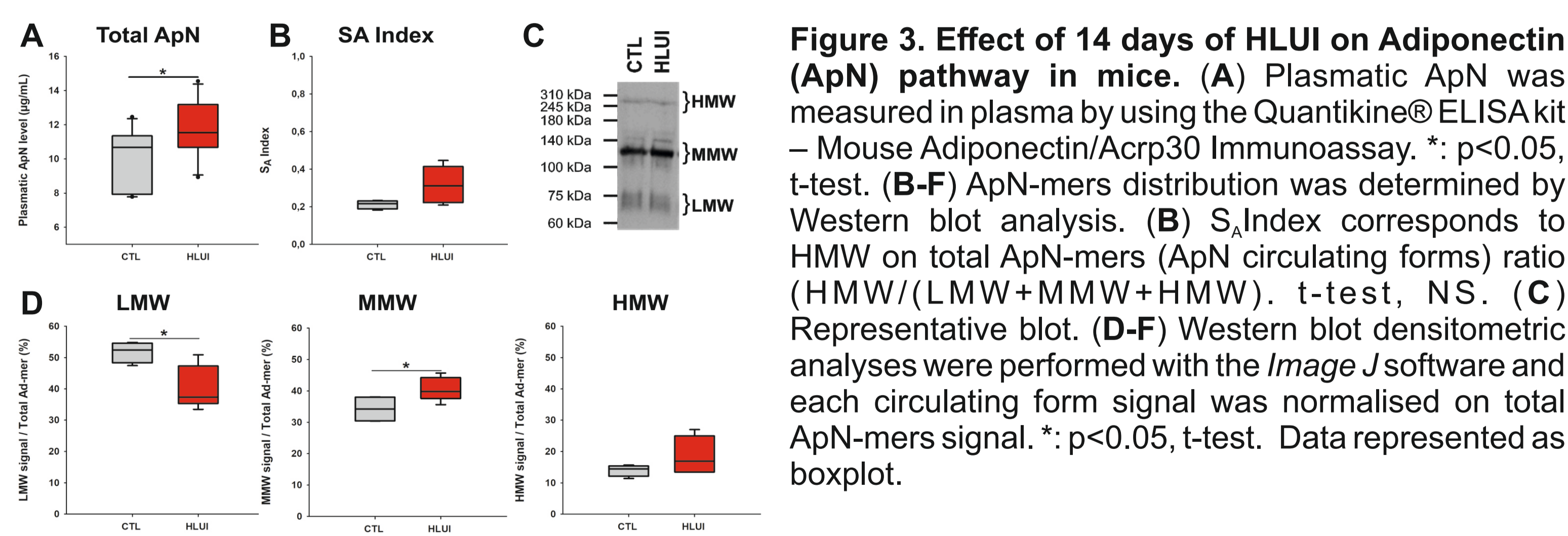
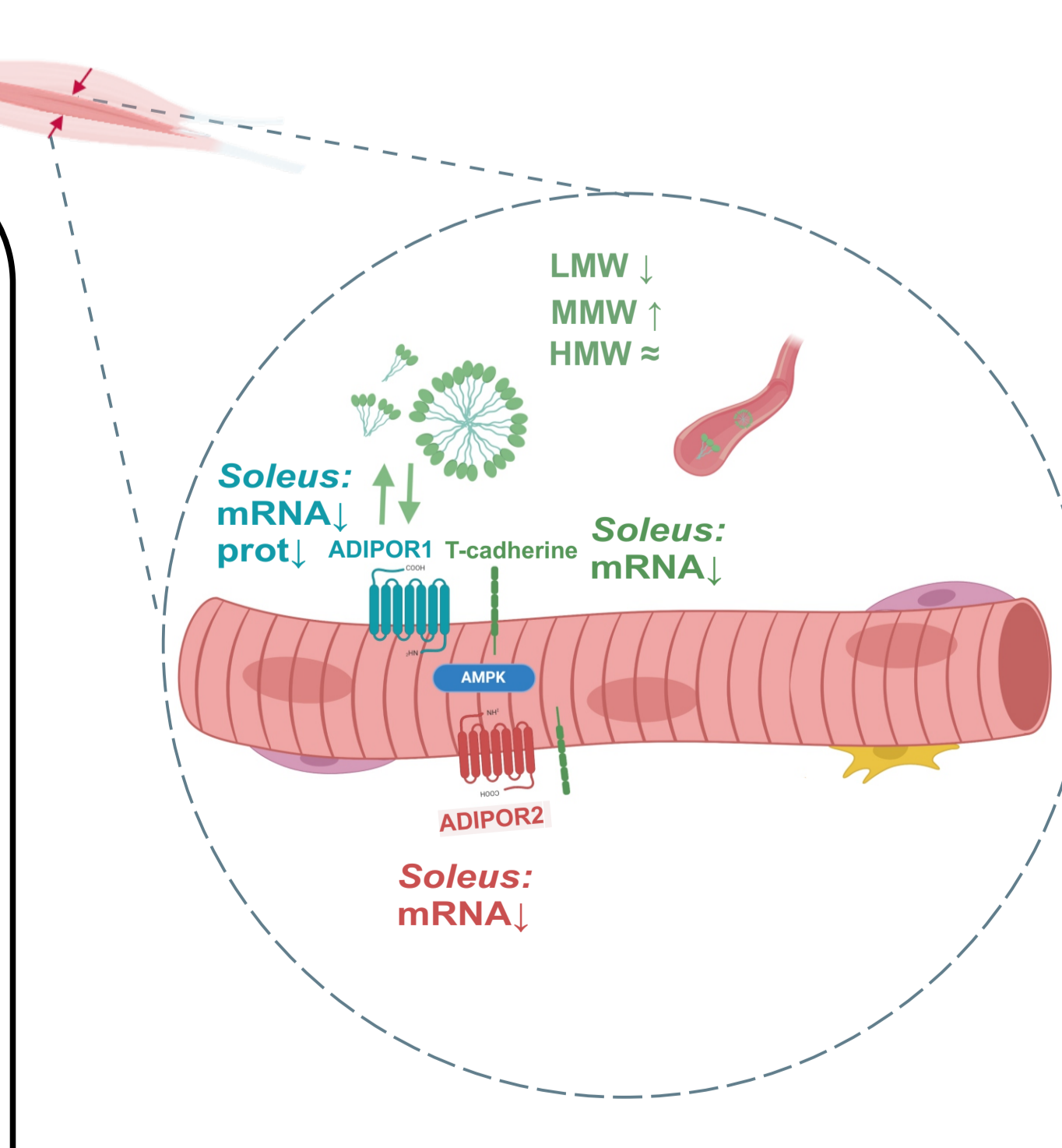


Figure 3. Effect of 14 days of HLUI on Adiponectin (ApN) pathway in mice. (A) Plasmatic ApN was measured in plasma by using the Quantikine® ELISA kit - Mouse Adiponectin/Acrp30 Immunoassay. *; $p < 0.05$, t-test. (B-F) ApN-mers distribution was determined by Western blot analysis. (B) S_{a} Index corresponds to HMW/(total ApN-mers (ApN) circulating forms) (HMW/(LMW+MMW+HMW)). t-test, NS. (C) Representative blot. (D-F) Western blot densitometric analyses were performed with the *Image J* software and each circulating form signal was normalised on total ApN-mers signal. *; $p < 0.05$, t-test. Data represented as boxplot.

Conclusions

In conclusion, we optimized a model allowing to mimic a moderated DMA in mouse hindlimb muscles (HLUI). In this model, modifications in myofibres CSA distribution and the decreased Feret's diameter indicates that effects are fibre type-dependent. Regarding plasmatic components of Adiponectin (ApN) pathway, the proportion of LMW circulating forms is decreased in HLUI mice in favor of MMW multimers. Total ApN plasmatic level is increased. Importantly, ApN pathway was also found altered in the disused *Soleus* slow-twitch muscle of HLUI mouse. ApN receptors and coreceptors mRNA expression are reduced in this muscle as well as *Adipor1* protein level. Such ApN pathway alterations were not observed in the *Tibialis Anterior* fast-twitch muscle (data not shown), suggesting that those alterations are fibre type-dependant.



Preliminary results in ApN-KO and WT mice submitted to HLUI suggest a more severe HLUI-mediated muscle atrophy in ApN-KO mice. Interestingly, RL and ET successfully induced muscle recovery after disuse.

Prospects

Ongoing studies aim to investigate whether ApN pro-myogenic effects are conserved in a disused muscle through gain and loss of function experiments associated with a muscle regeneration model.

If ApN pro-myogenic effects are conserved, ApN will constitute a good therapeutic target to improve muscle mass and regeneration following DMA.